




# Nerve detection during surgery: optical spectroscopy for peripheral nerve localization

Gerrit C. Langhout<sup>1</sup>  · Koert F. D. Kuhlmann<sup>1</sup> · Michel W. J. M. Wouters<sup>1</sup> · Jos A. van der Hage<sup>1</sup> · Frits van Coevorden<sup>1</sup> · Manfred Müller<sup>2</sup> · Torre M. Bydlon<sup>2</sup> · Henricus J. C. M. Sterenborg<sup>3</sup> · Benno H. W. Hendriks<sup>2,4</sup> · Theo J. M. Ruers<sup>1,5</sup>

Received: 29 May 2016 / Accepted: 26 December 2017 / Published online: 2 February 2018  
© Springer-Verlag London Ltd., part of Springer Nature 2018

## Abstract

Precise nerve localization is of major importance in both surgery and regional anesthesia. Optically based techniques can identify tissue through differences in optical properties, like absorption and scattering. The aim of this study was to evaluate the potential of optical spectroscopy (diffuse reflectance spectroscopy) for clinical nerve identification in vivo. Eighteen patients (8 male, 10 female, age  $53 \pm 13$  years) undergoing inguinal lymph node resection or resection of a soft tissue tumor in the groin were included to measure the femoral or sciatic nerve and the surrounding tissues. In vivo optical measurements were performed using Diffuse Reflectance Spectroscopy (400–1600 nm) on nerve, near nerve adipose tissue, muscle, and subcutaneous fat using a needle-shaped probe. Model-based analyses were used to derive verified quantitative parameters as concentrations of optical absorbers and several parameters describing scattering. A total of 628 optical spectra were recorded. Measured spectra reveal noticeable tissue specific characteristics. Optical absorption of water, fat, and oxy- and deoxyhemoglobin was manifested in the measured spectra. The parameters water and fat content showed significant differences ( $P < 0.005$ ) between nerve and all surrounding tissues. Classification using  $k$ -Nearest Neighbor based on the derived parameters revealed a sensitivity of 85% and a specificity of 79%, for identifying nerve from surrounding tissues. Diffuse Reflectance Spectroscopy identifies peripheral nerve bundles. The differences found between tissue groups are assignable to the tissue composition and structure.

**Keywords** Nerves · Nerve sparing · Surgery · Anesthesia · Optical spectroscopy · Spectroscopy

## Introduction

Precise nerve localization is of major importance in both surgery and regional anesthesia. Although postoperative neural

injury to large nerves is not extremely common, injury to smaller nerves like the parasympathetic nerve fibers in pelvic surgery can lead to disturbances in bladder function and sexual function in up to 30% of the patients [1, 2]. In regional anesthesia, the onset and quality of peripheral nerve blocks rely on the adequate placement of the anesthetics around the nerve. Several techniques have been investigated to facilitate nerve localization, including electrical and mechanical stimulation as well as ultrasound. Still, the success rate of regional anesthesia (complete sensory loss) using these guiding tools is limited to 63–81% [3–6]. Nerve stimulation is often not reliable, even when handled perfectly, as it requires neural conduction and a corresponding muscle response.

Diffuse Reflectance spectroscopy (DRS) is a technique capable of tissue identification, based on differences in optical tissue properties. When the tissue is illuminated through optical fibers in direct contact with the tissue, interaction of the light with tissue results in either absorption or scattering/reflection of the light. As absorption and scattering are tissue specific, illuminating tissue with a

✉ Gerrit C. Langhout  
N.langhout@nki.nl

<sup>1</sup> Department of Surgery, The Netherlands Cancer Institute, Antoni van Leeuwenhoek Hospital, Plesmanlaan 121, 1066 CX Amsterdam, The Netherlands

<sup>2</sup> Philips Research, In-Body Systems Department, HTC 34, 5656 AE Eindhoven, The Netherlands

<sup>3</sup> Department of Biomedical Engineering and Physics, Amsterdam Medical Center, Meibergdreef 9, 1105 AZ Amsterdam, The Netherlands

<sup>4</sup> Department of Biomechanical Engineering, Delft University of Technology, Mekelweg 2, 2628 CD Delft, The Netherlands

<sup>5</sup> Nanobiophysics Group, MIRA Institute, University of Twente, Post Box 217, 7500 AE Enschede, The Netherlands

selected spectral band of light and subsequent analysis of the characteristic scattering and absorption patterns will result in an “optical fingerprint” of the tissue [7]. Analytical models are able to extract biochemical, morphological, and physiological parameters from the measured spectra. In this way, DRS was able to identify nerve tissue in swine [7–9]. In contrast to nerve stimulation, optical spectroscopy does not rely on the effect on innervated muscle fibers and is therefore not hampered when the patient’s muscle function is reduced by anesthesia or when targeting sensory nerves or the autonomic nervous system.

The use of optical techniques for the detection of nerve tissue has recently been assessed in humans [10–12]. Post-mortem, in fresh frozen human bodies, nerves were detected with a sensitivity and specificity of around 90% [12]. The *in vivo* human study by Balthasar et al. [10] targeted six different nerves and distinguished three types of tissue (subcutaneous fat, muscle, and a combined group of near nerve adipose tissue and nerve) based on two parameters related to lipids and hemoglobin. Balthasar performed transcutaneous measurements using a needle-shaped optical stylus. Ultrasound was used as gold standard to determine needle position. Significant differences in parameter values were found between subcutaneous fat, muscle, and a region denominated as target region for regional anesthesia [10]. Because no classification was performed, no sensitivity and specificity was presented. Schols et al. used optical spectroscopy in the context of the development of a multispectral camera system. The study compared two types of detectors using optical spectroscopy *in vivo* in human. Nerve and adipose tissue could be differentiated with accuracies between 67 and 100% depending on classification method and sensor type [11]. The aim of the present study was to further investigate the potential of DRS to discriminate nerve tissue from multiple surrounding tissues *in vivo*. To test the hypothesis that nerve tissue could be discriminated from multiple surrounding tissue *in vivo*, we present differences in optical parameter values and perform a formal classification.

## Material and methods

This study was performed at The Netherlands Cancer Institute—Antoni van Leeuwenhoek hospital under approval of the protocol and ethics review board (NL40893.031.12). Written informed consent was obtained from all subjects. Patients undergoing inguinal lymph node dissection or resection of a soft tissue tumor located in the groin were included. Patients were selected based on the likelihood of exposure of the femoral or sciatic nerve. The exclusion of patients is visualized in Fig. 1.

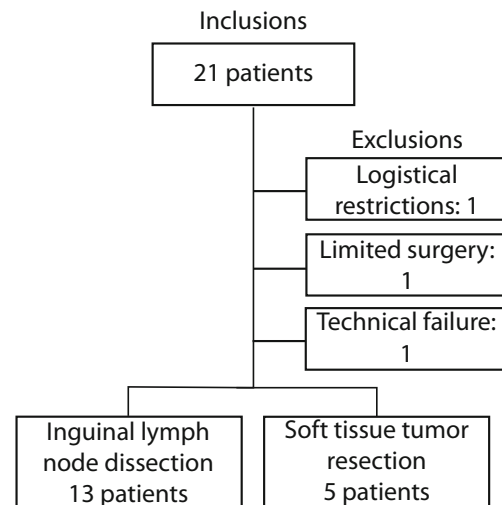


**Fig. 1** Three patients were excluded. In two cases, no measurements were performed due to logistical problems and unexpected extensive disease leading to conversion to restricted surgery. In one patient, the measurement results were strongly influenced by a separate light source. Eighteen patients remained, 15 on the femoral nerve, and three on the sciatic nerve

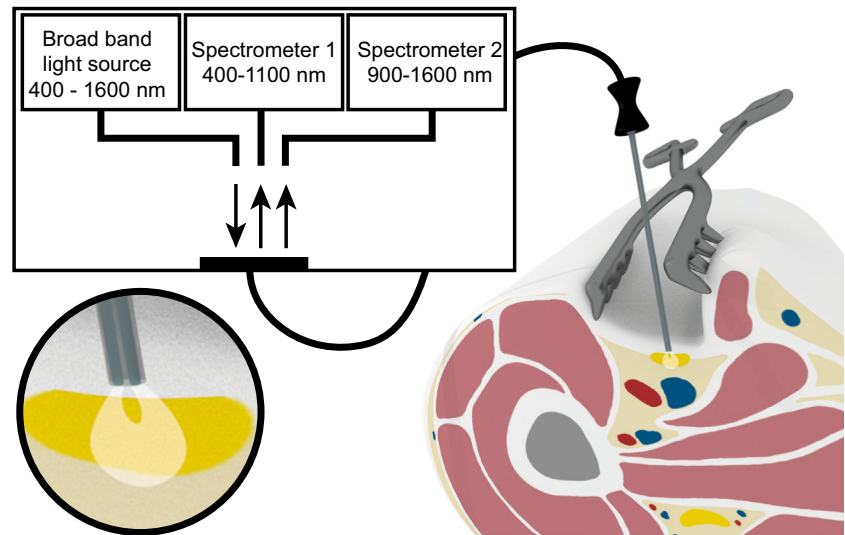
## Instrumentation

The instrumentation and calibration procedure of our optical spectroscopy system and validation of the quantifications of chromophores has been described elsewhere [13, 14]. A sterile probe containing two optical fibers (one illumination fiber and one collecting fiber, type N6, Invivo Germany, Schwerin, Germany) was used to deliver broad spectrum light from a tungsten-halogen source with integrated shutter (AvaLight HAL-S-IND 20 W, Avantes, Apeldoorn, The Netherlands). The diffusely reflected light, measured via the collecting fiber, was analyzed in the range of 400–1600 nm by two spectrometers (400 up to 1100 nm: DU420A-BRDD, 900 up to 1700 nm: DU492A-1.7 Andor Technology, Belfast, Northern Ireland) covering the visible and near-infrared ranges. In the present study, the distance between the illumination and collection fibers was 0.8 mm; the probe diameter at the tip was 1.9 mm. The setup is schematically represented in Fig. 2. The measurement setup is controlled by a custom-made LabView software interface (LabView, National Instruments, Austin, TX, USA).

## Measurements

Optical measurements were performed on nerve tissue, near-nerve adipose tissue, skeletal muscle, and subcutaneous fat. To guarantee the correct measurement location and close contact with the tissue of interest, optical measurements were performed under direct vision during open surgery. After exposure of the nerve, the blunt tip of the probe was placed on the nerve tissue by the surgeon. Blood collections were wiped

**Fig. 2** Scheme of measurement setup. The leg is visualized as cross-section with the optical probe placed on the femoral nerve. The round inlay shows a close-up of the tip of the probe



away before the measurements. At each measurement location (on-nerve, near-nerve adipose tissue, skeletal muscle, and subcutaneous fat), repeated measurements were processed and averaged to one measurement per location. During the recording, the surgical lights were dimmed to minimize the influence of environmental light.

### Spectral analysis

Tissue interactions with light are categorized as either optical absorption by chromophores or scattering, where scattering is the redirection of light by the particles in tissue. Each biological tissue has intrinsic absorption and scattering properties depending on the wavelength of light. Therefore, a tissue specific spectrum is measured during DRS. A widely accepted model, first described by Farrell et al., was used to quantify parameters related to the physiological, morphological, and metabolic characteristics of the measured tissue [15]. These parameters include volume fractions or concentrations of the different tissue chromophores and scattering parameters. The implementation of this model in Matlab (Matworks Inc., Natick, MA, USA) to analyze the diffuse reflectance spectra over a wavelength of 400–1600 nm is described by Nachabé et al. [16]. As the model was originally based on large fiber distances ( $> 1.5$  mm), over-estimation of specific parameters, such as water, fat,  $\beta$ -carotene, and hemoglobin, is inevitable [16]. A correction was applied by dividing these values by the mean of water plus fat content as measured in muscle and subcutaneous fat. Spectra highly contaminated by blood (hemoglobin concentration  $> 20\%$ ) were excluded from the analyses.

### Tissue classification and statistics

Tissue was classified according to the  $k$ -Nearest Neighbor (knn) principle with  $k = 3$ . In this test, the data is distributed between two sets (training and validation); a measurement is

classified as the most common class of three measurements with the best comparable values from the training set. Input for the algorithm were parameters derived from the DRS spectra: water content, fat content,  $\beta$ -carotene content, Mie scatter slope, scattering at 800 nm, hemoglobin concentration, and oxygen saturation. Parameters were normalized to a mean value of zero with a standard deviation of one, to give parameters an equal weight. A basic classification was done using a cross-validation method, i.e., subsequently taking out the spectra of one patient as the validation set and using the remaining spectra for training. The result of this classification is an estimation of the sensitivity, specificity, and Matthews correlation coefficient (MCC). This coefficient is used in machine learning as a measure of quality of classifications [17]. A MCC of +1 represents a perfect prediction and  $-1$  indicates total disagreement between prediction and observation.

### Results

Eighteen patients (8 male, 10 female) were included; 13 patients were scheduled for inguinal lymph node dissection and five for resection of a soft tissue tumor. Mean age of the patients was  $53 \pm 13$  years. A total of 628 measurements was performed, 295 on nerve, 101 on near-nerve adipose tissue, 124 on muscle, and 108 on subcutaneous fat. Nerve branches were measured ranging from 1 to 13 mm in diameter ( $5.7 \pm 3$  mm, mean  $\pm$  standard deviation). No extensive preparation of the nerves was performed, other than necessary for adequate surgery. All measured nerves were macroscopically identified by the surgeon.

### Spectra

An example of an optical measurement is seen in Fig. 3. The photograph shows the surgical area with the probe positioned

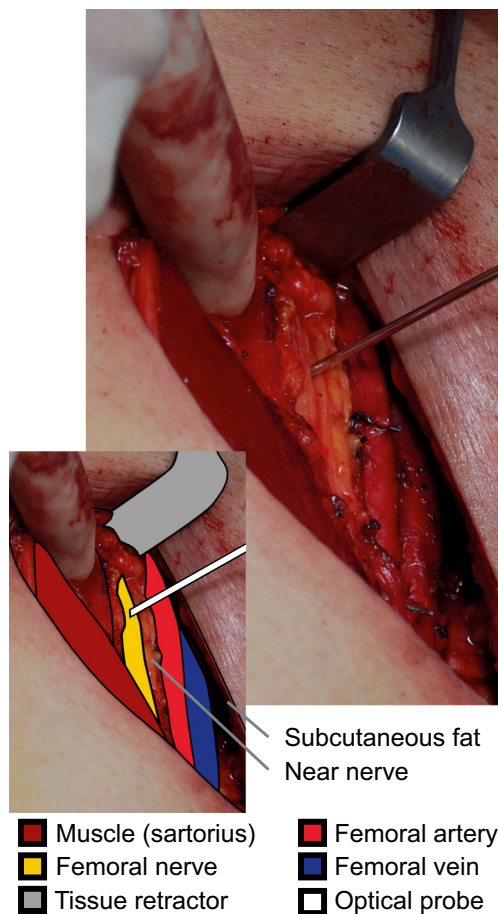


**Fig. 3** Photograph during a measurement, tissue types are indicated in the photo inset. The optical probe is positioned on the femoral nerve

on the femoral nerve. Measured spectra (Fig. 4) reveal optical characteristics of the investigated tissues. Typical examples of optical characteristics are the decrease in signal intensity (sharp dip) around 1200 nm due to lipid absorption (recognized in the spectra of subcutaneous fat and near-nerve adipose tissue). Optical absorption by water is recognized by multiple absorption peaks in the (near) infrared range, recognized in the graphs as sharp dips in measured light intensity. The water-related absorption peak at 1455 nm is most prominent in the spectra measured on muscle and nerve where the measured intensity is almost zero at 1400–1500 nm. Both oxygenated and deoxygenated hemoglobin were observed in all spectra, seen as a decrease in the signal intensity in the range of 400–600 nm.

### Tissue parameters

Box plots were generated based on all of the analyzed data (Fig. 5). Parameters strongly influenced by the visible part of the spectrum are grouped separately from the parameters derived from the infra-red part of the spectrum. The concentration of water is highest in muscle and low in adipose tissue.

The estimated concentration of fat is highest for measurements on subcutaneous fat, followed by near-nerve adipose tissue. Nerve measurements show high-fat levels compared to muscle but lower compared to subcutaneous fat. Fat and water parameters can be combined into the fat fraction ( $\text{fat}/(\text{fat} + \text{water})$ ). The average level of scattering in muscle is significantly lower compared to nerve. Blood levels are highest on muscle and comparable between subcutaneous fat and near-nerve adipose tissue and nerve. The blood saturation and beta-carotene levels are lower in muscle compared to on-nerve measurements.

### Tissue identification results

Although several parameters show significant differences between tissue groups, optimal tissue identification was based upon the interrelationship of multiple parameters using a classification algorithm. 3-Nearest-Neighbor classification using a subset of parameters revealed an MCC of 0.64 (values above zero indicate a positive correlation) with a sensitivity of 85% and a specificity of 79%. Parameters selected for the subset were the concentrations of hemoglobin and fat, oxygen saturation, fat fraction ( $\text{fat}/(\text{fat} + \text{water})$ ), and two scattering parameters: scattering at 800 nm and the scatter slope. Selection of these parameters was based on the impact on the MCC of all measurements when systematically excluding parameters used in the classification tree.

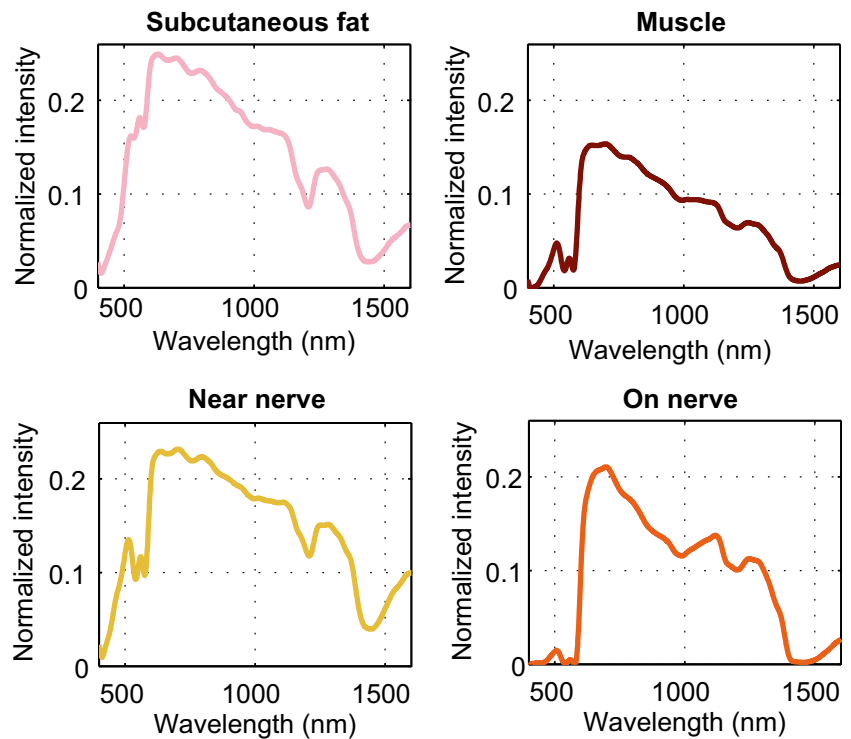
### Discussion

This in vivo human study shows the potential of DRS to identify nerve tissue. Remarkable differences in optical spectra exist between nerve and various surrounding tissues. Within a classification algorithm, the most valuable parameters for nerve tissue discrimination were hemoglobin and fat concentration, fat fraction, oxygen saturation, and scattering parameters. Nerve tissue could be detected with a sensitivity and specificity of 85 and 79%, respectively. Compared to the results of previous studies, the changes in fat concentration from subcutaneous fat to muscle and nerve are remarkably similar compared to Balthasar [10]. In contrast to Balthasar, we found larger concentrations hemoglobin in nerve compared to subcutaneous fat. Balthasar used a sharp needle with a transcutaneous approach; piercing of the skin might result in bleeding as cause of a higher hemoglobin concentration in subcutaneous fat.

Heterogeneity of nerves and their composition may challenge automatic identification. The morphology and chemical composition differ per nerve (e.g., femoral nerve or sciatic nerve) and even depend on the position on the nerve [18]. An example of the heterogeneity of composition of nerves is the amount of intraneural adipose tissue. This amount varies



**Fig. 4** Typical examples of the measured spectra per tissue class depicted as the normalized intensity of the reflected light as a function of the wavelength



between nerves and the position on the nerve (proximal or distal) [18]. In small nerve branches, the epineurium is fused with the perineurium, eliminating the space for intraneural adipocytes [19]. In this study, a variety of nerve branches was included. Measurements were performed on nerve branches with diameters ranging from 1 to 13 mm, from two different nerve types. In a specific clinical setting, the target

nerve location will be more specified which will limit the variation in nerve diameter, composition and morphology, and hence lower the variability in the optical properties. It is expected that this will enhance the performance of optical nerve identification.

For clinical applications in a defined anatomical region, the probed volume of DRS can be tailored to a specific

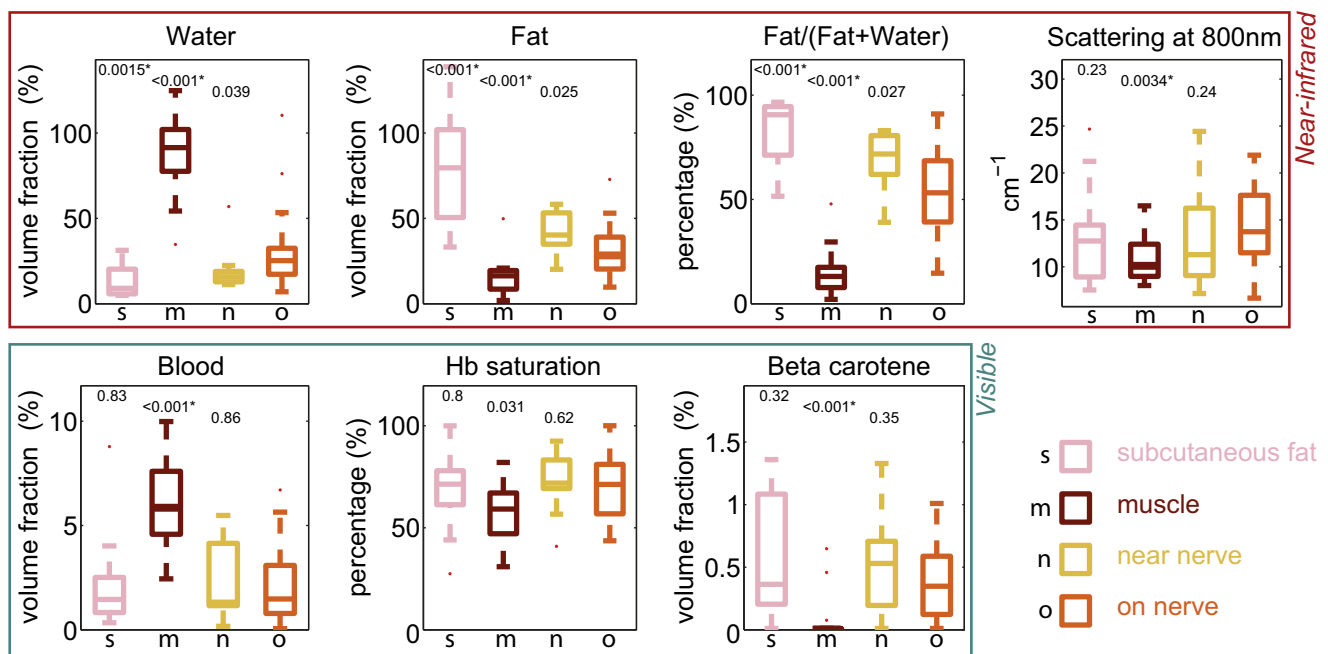


**Fig. 5** Box plots of relevant tissue parameters. The significance levels depicted above the bars indicate the difference ( $p$  value) between the tissue and the nerve tissue based on a Mann-Whitney  $U$  test

application. The probed volume is influenced by the distance between the illuminating and the collecting fiber. When the inter-fiber distance is increased, light travels a longer path through the tissue. This leads to an increased probed volume as well as an increased penetration depth [20]. In a defined anatomical region or a specific clinical application, less variation in the nerve diameter will be encountered thereby allowing a device with the most optimal inter-fiber distance to be selected.

Open surgery was used as gold standard for anatomical identification. After a process with careful preparation and exposure, using the surgeons experience, anatomical knowledge, and sight, the nerve could be identified with maximum certainty, this applies in particular for the larger nerves selected in this study. The maximum advantage of a nerve identification technique during surgery would be during or prior to extensive preparation, especially in situations where anatomical relations are distorted or when visible of tactile feedback is limited. In addition, in the current setting, the surface was wiped before the measurements to remove blood collections. However, due to small bleedings, some variability in the blood content may still have been present due to these bleedings. A potential advantage of our method of analyzing the spectra is that the individual chromophores can be quantified separately which increases the robustness of the technique while improving clinical comprehension. For example, in regional anesthesia, the nerve is approached with a needle meaning that the tissue is not exposed to air. Our approach may take into account such differences in application by prioritizing the individual parameters. In this case, the oxygen saturation could be left out of the classification algorithm.

The DRS technology, here assembled in a measurement probe, could also be incorporated into needles for regional anesthesia or surgical instruments. DRS stylets, compatible with a 20-gauge needle cannula, were already used in swine and human [8, 10]. The diameter of the optical fibers (200  $\mu\text{m}$ ) used in the probes for this study could also easily be fitted into surgical dissection tools or needles used for regional anesthesia application.

## Conclusion

Optical spectroscopy with the use of DRS allows for identification of nerve tissue based on both differences in clinical comprehensive parameters as well as on formal automated classification. The differences found between tissue groups are assignable to the tissue composition and structure and may be valuable in nerve detection or localization in regional anesthesia or surgical procedures.

**Acknowledgements** We would like to thank Arnold van Keersop (Philips Research) for his assistance in analyzing the data and Vishnu Pully and Christian Reich for technical support during the data collection. We

acknowledge Marjolein van der Voort and Gerald Lucassen (Philips Healthcare) for their guidance in the overall study design, data analysis, and review of the manuscript.

**Funding information** For this study, The Netherlands Cancer Institute received an unrestricted grant from Philips Research. This research was further supported by a grant of the KWF-Alpe d’HuZes (NKI 2014-6596).

## Compliance with ethical standards

**Conflict of interest statement** The authors who are affiliated with Philips Research (M.M., T.B., B.H.) are employees of Philips. The prototype system described in this article is a research prototype. None of the other authors have any conflicts of interest.

**Ethical approval** This study was performed at The Netherlands Cancer Institute—Antoni van Leeuwenhoek hospital under approval of the protocol and ethics review board (NL40893.031.12).

**Informed consent** Written informed consent was obtained from all individual participants included in the study.

## References

1. Lange MM, van de Velde CJ (2010) Long-term anorectal and urogenital dysfunction after rectal cancer treatment. *Sem Col Rec Surg*, pp 87–94
2. Celentano V, Fabbrocile G, Luglio G, Antonelli G, Tarquini R, Bucci L (2010) Prospective study of sexual dysfunction in men with rectal cancer: feasibility and results of nerve sparing surgery. *Int J Color Dis* 25:1441–1445
3. Urmev WF, Stanton J (2002) Inability to consistently elicit a motor response following sensory paresthesia during interscalene block administration. *Anesthesiology* 96:552–554
4. Perlas A, Niazi A, McCartney C, Chan V, Xu D, Abbas S (2006) The sensitivity of motor response to nerve stimulation and paresthesia for nerve localization as evaluated by ultrasound. *Reg Anesth Pain Med* 31:445–450
5. Walker KJ, McGrattan K, Aas-Eng K, Smith AF (2009) Ultrasound guidance for peripheral nerve blockade. *Cochrane Db Syst Rev* 4: CD006459
6. Chan VW, Perlas A, McCartney CJ, Brull R, Xu D, Abbas S (2007) Ultrasound guidance improves success rate of axillary brachial plexus block. *Can J Anaesth* 54:176–182
7. Brynolf M, Sommer M, Desjardins AE, van der Voort M, Roggeveen S, Bierhoff W, Hendriks BH, Rathmell JP, Kessels AG, Söderman M (2011) Optical detection of the brachial plexus for peripheral nerve blocks: an in vivo swine study. *Reg Anesth Pain Med* 36:350–357
8. Desjardins AE, Van der Voort M, Roggeveen S, Lucassen G, Bierhoff W, Hendriks BH, Brynolf M, Holmström B (2011) Needle stylet with integrated optical fibers for spectroscopic contrast during peripheral nerve blocks. *J Biomed Opt* 16:077004
9. Stelzle F, Knipfer C, Bergauer B, Rohde M, Adler W, Tangermann-Gerk K, Nkenke E, Schmidt M (2014) Optical nerve identification in head and neck surgery after Er: YAG laser ablation. *Lasers Med Sci* 29:1641–1648
10. Balthasar A, Desjardins AE, van der Voort M, Lucassen GW, Roggeveen S, Wang K, Bierhoff W, Kessels AG, van Kleef M, Sommer M (2012) Optical detection of peripheral nerves: an in vivo human study. *Reg Anesth Pain Med* 37:277–282

11. Schols RM, ter Laan M, Stassen LP, Bouvy ND, Amelink A, Wieringa FP, Alic L (2014) Differentiation between nerve and adipose tissue using wide-band (350–1,830 nm) in vivo diffuse reflectance spectroscopy. *Laser Surg Med* 46:538–545
12. Hendriks BH, Balthasar AJ, Lucassen GW, van der Voort M, Mueller M, Pully VV, Bydlon TM, Reich C, van Keersop AT, Kortsmid J, Langhout GC, van Geffen GJ (2015) Nerve detection with optical spectroscopy for regional anesthesia procedures. *J Trans Med* 13:380
13. Nachabé R, Evers DJ, Hendriks BH, Lucassen GW, van der Voort M, Rutgers EJ, Peeters M-JV, Van der Hage JA, Oldenburg HS, Wesseling J (2011) Diagnosis of breast cancer using diffuse optical spectroscopy from 500 to 1600 nm: comparison of classification methods. *J Biomed Opt* 16:087010–087012
14. Nachabé R, Sterenberg HJ, Hendriks BH, Desjardins AE, van der Voort M, van der Mark MB (2010) Estimation of lipid and water concentrations in scattering media with diffuse optical spectroscopy from 900 to 1600 nm. *J Biomed Opt* 15:037015
15. Farrell TJ, Patterson MS, Wilson B (1992) A diffusion theory model of spatially resolved, steady-state diffuse reflectance for the noninvasive determination of tissue optical properties in vivo. *Med Phys* 19:879–888
16. Nachabé R, Hendriks BH, van der Voort M, Desjardins AE, Sterenberg HJ (2010) Estimation of biological chromophores using diffuse optical spectroscopy: benefit of extending the UV-VIS wavelength range to include 1000 to 1600 nm. *Biomed Opt Express* 1:1432–1442
17. Getoor L, Taskar B (2007) Introduction to statistical relational learning. MIT press, London
18. Maravilla KR, Bowen BC (1998) Imaging of the peripheral nervous system: evaluation of peripheral neuropathy and plexopathy. *Am J Neuroradiol* 19:1011–1023
19. Brady S, Siegel G, Albers RW, Price D (2007) Basic neurochemistry: molecular, cellular and medical aspects, 7th edn. Elsevier Academic Press, Burlington
20. Arifler D, MacAulay C, Follen M, Richards-Kortum R (2006) Spatially resolved reflectance spectroscopy for diagnosis of cervical precancer: Monte Carlo modeling and comparison to clinical measurements. *J Biomed Opt* 11:064027